

Recursion scheme for the largest β -Wishart-Laguerre eigenvalue and Landauer conductance in quantum transport

Peter J. Forrester*

*School of Mathematics and Statistics, ARC Centre of Excellence for Mathematical and Statistical Frontiers,
The University of Melbourne, Victoria 3010, Australia*

Santosh Kumar†

Department of Physics, Shiv Nadar University, Uttar Pradesh 201314, India

The largest eigenvalue distribution of the Wishart-Laguerre ensemble, indexed by Dyson parameter β and Laguerre parameter a , is fundamental in multivariate statistics and finds applications in diverse areas. Based on a generalization of the Selberg integral, we provide an effective recursion scheme to compute this distribution explicitly in both the original model, and a fixed-trace variant, for a, β non-negative integers and finite matrix size. For $\beta = 2$ this circumvents known symbolic evaluation based on determinants which become impractical for large dimensions. Our exact results have immediate applications in the areas of multiple channel communication and bipartite entanglement. Moreover, we are also led to the exact solution of a long standing problem of finding a general result for Landauer conductance distribution in a chaotic mesoscopic cavity with two ideal leads. Thus far, exact closed-form results for this were available only in the Fourier-Laplace space or could be obtained on a case-by-case basis.

Introduction.— The Wishart-Laguerre ensemble constitutes an important class of random matrices and has been of immense usefulness in modeling a variety of problems in diverse topics [1–3]. The corresponding extreme eigenvalues, aside from being fundamental in multivariate statistics [1, 4–15], play crucial roles in problems ranging from quantum entanglement in bipartite systems [16–19], and electronic transport properties in mesoscopic systems [10, 20], to multichannel communication in wireless networks [21–29]. The asymptotic behavior of these extreme eigenvalues and the corresponding gap probabilities have been explored extensively, leading to Tracy-Widom densities [12, 13, 30–33] and large-deviation results [34–37] of significant importance. In certain applications, however, one requires to go beyond universal results and seek exact and explicit computation of these distributions for finite matrix size. Typical theory in this connection is based on determinants or Pfaffians requiring symbolic computation [6, 10, 11, 14, 15, 26], and therefore becomes impractical to evaluate if large matrices are involved. An alternative approach for obtaining explicit expressions involves implementing certain recurrences. This has turned out to be very effective considering the availability of modern software packages which can handle recursive symbolic computation very efficiently. For the smallest eigenvalue of real Wishart-Laguerre matrices, in Refs. [38, 39] Edelman provided a recursion scheme which has subsequently been generalized to other ensembles and symmetry classes [1, 10, 19, 40–44]. However, extending this to the largest eigenvalue distribution has remained elusive due to its comparatively more convoluted mathematical structure [1].

In this work, we accomplish the task of providing an efficient recursion scheme for evaluating the probability

density function (PDF) as well as the cumulative distribution function (CDF) of the largest eigenvalue of the integer β -Wishart-Laguerre ensemble for both unrestricted and fixed trace variants. These results apply at once to problems pertaining to multiple channel communication in wireless systems and bipartite entanglement in random pure states. Additionally, we exploit the connection of the largest eigenvalue of the fixed trace Wishart-Laguerre ensemble to the quantum conductance problem and solve a long-standing problem of obtaining a general closed-form result for the Landauer conductance distribution in a chaotic mesoscopic cavity with ideal leads. Thus far, exact closed-form results for this distribution were available only in the Fourier-Laplace space as a determinant or could be obtained on a case by case basis [45–51].

To present our findings, we begin by providing the general results for the functional form of the PDF and CDF of the Wishart-Laguerre largest eigenvalue, along with a brief discussion of their immediate applicability to the multiple channel communication and bipartite entanglement problems. We then briefly describe the machinery behind our proposed recursive approach and also present comparison of analytical and Monte Carlo simulation based results for a few examples. The application to the quantum conductance problem is discussed next, where we point out the implementation of recursion scheme to obtain exact Landauer conductance distribution. The analytical results in this case are contrasted with the numerical results obtained with the aid of scattering matrices modeled using circular ensemble of random matrices. Finally, we conclude with a brief summary of our work.

Exact distribution for the β -Wishart-Laguerre largest eigenvalue. — The classical cases of Wishart-Laguerre ensemble include real, complex and quaternion positive-

definite matrices of the form WW^\dagger , designated by the Dyson index $\beta = 1, 2$ and 4 , respectively. In recent years, matrix models for continuous $\beta > 0$ variants have been also worked out and have drawn considerable attention. In the general case, the joint PDF for Wishart-Laguerre eigenvalues ($0 < x_1, \dots, x_n < \infty$) is given by

$$\mathcal{P}(x_1, \dots, x_n) = \frac{1}{W} \prod_{l=1}^n x_l^a e^{-\beta x_l/2} \prod_{1 \leq j < k \leq n} |x_k - x_j|^\beta, \quad (1)$$

with $a > -1$. The partition function W is known using the Selberg integral as [1, 2]

$$W = \left(\frac{2}{\beta}\right)^\gamma \prod_{j=0}^{n-1} \frac{\Gamma\left(\frac{\beta(j+1)}{2} + 1\right) \Gamma\left(\frac{\beta(j+a)}{2} + 1\right)}{\Gamma\left(\frac{\beta}{2} + 1\right)}, \quad (2)$$

where $\gamma = n[a + \beta(n-1)/2 + 1]$. The PDF and CDF of the largest eigenvalue are computed as [1]

$$P(x) = n \int_0^x dx_2 \cdots \int_0^x dx_n \mathcal{P}(x, x_2, \dots, x_n), \quad (3)$$

$$Q(x) = \int_0^x dx_1 \cdots \int_0^x dx_n \mathcal{P}(x_1, \dots, x_n) = \int_0^x dx' P(x'). \quad (4)$$

The CDF of the largest eigenvalue coincides with the gap probability $E_{n,\beta}(0; (x, \infty))$ of finding no eigenvalue in the domain (x, ∞) .

We demonstrate below that for positive integer β and non-negative integer a , the sought PDF and CDF exhibit respective structures:

$$P(x) = \sum_{j=1}^n e^{-j\beta x/2} \sum_{k=a}^{ja+j(n-j)\beta} c_{jk} x^k, \quad (5)$$

$$Q(x) = \sum_{j=0}^n e^{-j\beta x/2} \sum_{k=0}^{ja+j(n-j)\beta} d_{jk} x^k. \quad (6)$$

For complex matrices ($\beta = 2$), the above structures have been pointed out in Ref. [22] in the context of multiple channel communication problem. However, the computation of the coefficients (which depend on β, a and n and evaluate to rational numbers) has remained a daunting task [22–24]. These earlier works have relied on evaluating the coefficients using the Hankel determinant of an n -dimensional matrix. This becomes prohibitive if n becomes large (say, $\gtrsim 10$). As we will see below, our recursive approach facilitates the evaluation of PDF, CDF and coefficients in an efficient manner.

The fixed-trace variant of the Wishart-Laguerre ensemble is described by the joint density

$$\begin{aligned} \mathcal{P}_F(y_1, \dots, y_n) &= \frac{1}{W_F} \delta\left(\sum_i y_i - 1\right) \prod_{l=1}^n y_l^a \\ &\times \prod_{1 \leq j < k \leq n} |y_k - y_j|^\beta, \end{aligned} \quad (7)$$

where the eigenvalues ($0 \leq y_1, \dots, y_n \leq 1$) are constrained by the Dirac-delta condition, and $W_F = [1/\Gamma(\gamma)](\beta/2)^\gamma W$ is the corresponding partition function. The PDF and CDF of the largest eigenvalue for this ensemble follows from the Fourier-Laplace relationship with the unrestricted trace variant [1], Eq. (1), as

$$\begin{aligned} P_F(y) &= \frac{2}{\beta} \Gamma(\gamma) \sum_{j=1}^n \Theta(1 - jy) \\ &\times \sum_{k=a}^{ja+j(n-j)\beta} \frac{c_{jk}}{\Gamma(\gamma - k - 1)} \left(\frac{2y}{\beta}\right)^k (1 - jy)^{\gamma - k}, \end{aligned} \quad (8)$$

$$\begin{aligned} Q_F(y) &= \Gamma(\gamma) \sum_{j=0}^n \Theta(1 - jy) \\ &\times \sum_{k=0}^{ja+j(n-j)\beta} \frac{d_{jk}}{\Gamma(\gamma - k)} \left(\frac{2y}{\beta}\right)^k (1 - jy)^{\gamma - k - 1}, \end{aligned} \quad (9)$$

where $\Theta(z)$ denotes the Heaviside step function. It should be noted that the largest eigenvalue in this case also coincides with the scaled largest eigenvalue associated with Eq. (1), i.e., $y_{\max} = x_{\max}/(x_1 + \cdots + x_n)$.

The above results apply directly to the multiple channel communication and bipartite entanglement problems. In multiple input multiple output (MIMO) communication, the channel matrix H is the central object. It models the fading of the signal between n_t and n_r number of transmitting and receiving antennas, respectively. The singular values of the $n_r \times n_t$ -dimensional H matrix or, equivalently, the eigenvalues of HH^\dagger (or $H^\dagger H$) play a crucial role in deciding several quantities of interest which assess the performance of the MIMO system. In the cases of one-sided Gaussian and Rayleigh fading, the eigenvalues are described by the density given in Eq. (1) with $\beta = 1$ and 2 , respectively, and the parameter $a = \beta(|n_t - n_r| + 1)/2 - 1$. In Ref. [22, 23], it has been shown within a transmit-beamforming model with maximum ratio combining (MRC) receivers that the maximum output signal-to-noise (SNR) is directly related to the largest eigenvalues of HH^\dagger . Consequently, the distribution of the largest eigenvalue has been used to obtain the statistics of symbol error probability (SEP), outage probability and ergodic channel capacity [22, 23]. Additionally, the distribution of the scaled largest eigenvalue finds applications in various hypothesis testing problems, both in statistics and in signal processing [24, 52–58].

In the problem of bipartite entanglement, one is interested in the properties of the reduced density matrix. To elaborate, consider Hilbert spaces $\mathcal{H}_n, \mathcal{H}_m$ of dimensions n and m for the constituents with $n \leq m$. Moreover, let $|\phi\rangle$ be a pure state belonging to the composite system, i.e., $|\phi\rangle \in \mathcal{H}_n \otimes \mathcal{H}_m$. In case $|\phi\rangle$ is chosen randomly in a uniform manner, the Schmidt eigenvalues of the reduced

density matrix $\rho = \text{tr}_m(|\phi\rangle\langle\phi|)$ obtained by partial tracing over the part belonging to \mathcal{H}_m are governed by the joint PDF Eq. (7) with $a = \beta(m - n + 1)/2 - 1$ [1, 59]. The largest of these eigenvalue varies from $1/n$ to 1. In these two extremes, owing to the fixed trace restriction, all other eigenvalues assume a common value of $1/n$ and 0, respectively. These respective scenarios correspond to the two subsystems being maximally entangled and separable. The distribution of the largest eigenvalue of the fixed trace ensemble therefore carries important information regarding the entanglement between the subsystems of the composite bipartite system [18].

Recursion scheme.— We now briefly describe the machinery behind the recursion scheme to obtain the CDF and PDF of the largest eigenvalue. To begin with, we will demonstrate that the multi-dimensional integral in Eq. (4) for $Q(x)$ does lead to the structure shown in Eq. (6). For even β , we expand $\prod_{j < k} |x_k - x_j|^\beta$ as a homogeneous multivariable polynomial of degree $\beta n(n - 1)/2$, viz.,

$$\prod_{1 \leq j < k \leq n} |x_k - x_j|^\beta = \sum_{\kappa=(\kappa_1, \dots, \kappa_n)} \alpha_\kappa \prod_{l=1}^n x_l^{\kappa_l}, \quad (10)$$

for some coefficients α_κ . Here κ is a partition involving up to n parts and of fixed length such that $\sum_{j=1}^n \kappa_j = \beta n(n - 1)/2$. With $\kappa_1 \geq \kappa_2 \geq \dots$, it is known $\kappa_j \leq (n - j)\beta$. Substituting the above expansion in Eq. (10) yields

$$Q(x) = \frac{1}{W} \sum_{\kappa} \alpha_\kappa \prod_{l=1}^n \left(\int_0^x dx_l x_l^{a+\kappa_l} e^{-\beta x_l/2} \right). \quad (11)$$

Provided a is a non-negative integer, the integral inside the above product can be evaluated as

$$\int_0^x ds s^a e^{-bs/2} = a! \left(\frac{2}{\beta} \right)^{a+1} \left[1 - e^{-\beta x/2} \sum_{k=0}^a \frac{1}{k!} \left(\frac{\beta x}{2} \right)^k \right]. \quad (12)$$

Therefore, eventually we wind up with the expansion of the form given in Eq. (6), but with the upper limit of the inner sum (over k) equal to $ja + j[n - (j + 1)/2]\beta$. As shown in the Appendix I, this can be refined to $ja + j(n - j)\beta$ as in Eq. (6). Also, Eqs. (11) and (12) imply that for β even $d_{j0} = (-1)^j \binom{n}{j}$. For handling odd β , we order the eigenvalues so that $x_1 > x_2 > \dots > x_n > 0$, and then the expansion in Eq. (10) is valid for appropriate coefficients α_κ . Moreover, the $Q(x)$ can be written as the iterated multi-dimensional integral $n! \int_0^x dx_1 \dots \int_0^{x_{n-2}} dx_{n-1} \int_0^{x_{n-1}} dx_n \mathcal{P}(x_1, \dots, x_n)$, leading again to Eq. (6). The expansion in Eq. (5) for the PDF $P(x)$ follows similarly by using Eqs. (10) and (12) in Eq. (3).

We next discuss a recursion scheme for the computation of the coefficients. We introduce the auxiliary

function, generalising the Laguerre weighted Selberg integral [1, 2]

$$L_{p,\nu}^{(\alpha)}(x) = \frac{p!(\nu - p)!}{\nu!} \int_0^x dt_1 \dots \int_0^x dt_\nu \prod_{l=1}^\nu t_l^{\lambda_l} e^{-\lambda_l t_l} |x - t_l|^\alpha \times \prod_{1 \leq j < k \leq \nu} |t_k - t_j|^{2\lambda} e_p(x - t_1, \dots, x - t_\nu), \quad (13)$$

where $e_p(t_1, \dots, t_\nu)$ are the elementary symmetric polynomials. At the heart of the recursion lies a remarkable linear differential-difference equation [42, 43],

$$\lambda(\nu - p) L_{p+1,\nu}^{(\alpha)}(x) = [\lambda(\nu - p)x + B_p] L_{p,\nu}^{(\alpha)}(x) + x \frac{d}{dx} L_{p,\nu}^{(\alpha)}(x) - D_p x L_{p-1,\nu}^{(\alpha)}(x), \quad (14)$$

where $p = 0, 1, \dots, \nu - 1$ and

$$B_p = (p - \nu)[\lambda_1 + \alpha + 1 + \lambda(\nu - p - 1)], \\ D_p = p[\lambda(\nu - p) + \alpha + 1].$$

Suppose $L_{0,\nu}^{(\alpha)}(x)$ is known. Application of the recurrence allows for the computation of $L_{\nu,\nu}^{(\alpha)}(x)$ which is identical to $L_{0,\nu}^{(\alpha+1)}(x)$. With $\nu = n$, $2\lambda = \beta$, iterating to the value $\alpha = \beta$ gives $Q(x)$.

The difficulty is that $L_{0,\nu}^{(\alpha)}(x)$ is known only for $\nu = 1$. Fortunately, the relation between $P(x)$ and $Q(x)$ displayed in Eq. (4) permits an iteration also in ν , as observed in a recursive computation of the largest eigenvalue PDF of the Gaussian orthogonal ensemble given by James [60]. Thus we begin with Eq. (12) to obtain $\int_0^x dx_1 x_1^a e^{-\beta x_1/2}$. The recurrence in Eq. (14) can then be applied β times to evaluate

$$\int_0^x dx_1 x_1^a e^{-\beta x_1/2} |x - x_1|^\beta.$$

Next, we denote x by x_2 in the above expression, multiply by $x_2^a e^{-\beta x_2/2}$, and integrate over x_2 from 0 to x to obtain

$$\int_0^x dx x_2^a e^{-\beta x_2/2} \int_0^{x_2} dx_1 x_1^a e^{-\beta x_1/2} |x_2 - x_1|^\beta,$$

which is the same as half this double-integral with the upper limit of the inner integral changed to x from x_2 . Now we essentially repeat this procedure. Using the recurrence, knowledge of the above two dimensional integral is used to compute

$$\int_0^x dx_2 x_2^a e^{-\beta x_2/2} \int_0^x dx_1 x_1^a e^{-\beta x_1/2} \prod_{1 \leq j < k \leq 3} |x_k - x_j|^\beta,$$

which is then multiplied by $x_3^a e^{-\beta x_3/2}$, and integrated over x_3 , and so on. Continuing, we eventually arrive at the expansion Eq. (6). An important point is that at all stages of the iteration the one-dimensional integral in

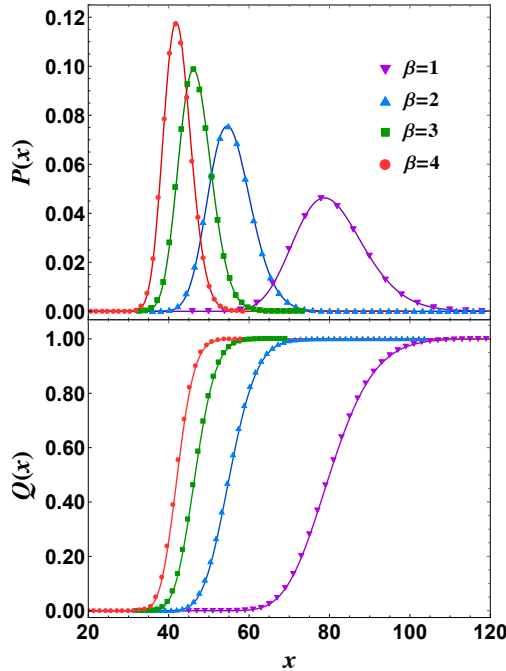


FIG. 1. PDF and CDF of the largest eigenvalue for the unrestricted trace Wishart-Laguerre ensemble for $n = 10, a = 15$.

Eq. (12) applies and the expressions can be written in an expansion analogous to Eq. (6). It should be also noted that the expansion for $P(x)$ appears in this procedure a step before the final integration is considered for $Q(x)$. Furthermore, when evaluating the expressions for a given n , the results for lower dimensions are also obtained in the process.

A Mathematica [61] code to implement the above described recursion scheme can be found in the Appendix II along with a brief description. It also extracts the coefficients c_{jk} and d_{jk} which can then be used for evaluating results for the fixed trace ensemble. As an example, we have considered $n = 10, a = 15$ and shown the plots for $\beta = 1, 2, 3, 4$ in Figs. 1 and 2. The analytical result based solid curves are contrasted against the numerical simulation based overlaid symbols and we can see an excellent agreement.

Exact distribution of Landauer conductance.— One of the remarkable achievements of random matrix theory (RMT) has been in the field of quantum conductance in chaotic mesoscopic systems [45–48, 62–65]. Starting from its prediction of universal conductance fluctuation [45, 46, 62–64] to the modern day description of topological superconductors and Majorana fermions [65], RMT has had great success in modeling various charge transport related phenomena. Despite this, there remain several problems which have defied an exact solution. One such problem is working out the exact distribution of Landauer conductance in a chaotic mesoscopic cavity with ideal leads [45–51]. Here we solve this problem

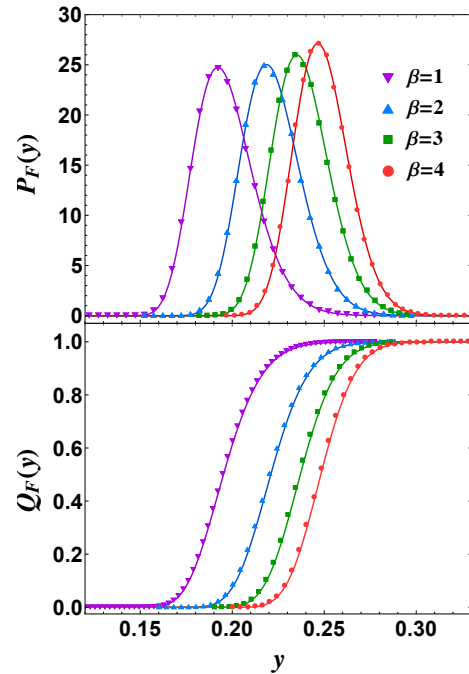


FIG. 2. PDF and CDF of the largest eigenvalue for the fixed trace Wishart-Laguerre ensemble for $n = 10, a = 15$.

by exploiting its mathematical connection with largest eigenvalue of the fixed trace Wishart-Laguerre ensemble.

The chaotic mesoscopic cavity is connected to an electron reservoir via two ideal leads. The electronic transport properties follow from the knowledge of the scattering matrix (S matrix). In this case, the S matrix can be modeled using Dyson's circular ensemble [45–47, 66] (note that for nonideal leads the S -matrix has to be taken from a nonuniform measure given by the Poisson kernel [1, 45, 67, 68]). For given number of channels n_1 and n_2 in the two leads, the S matrix is $n_1 + n_2$ dimensional. The Landauer conductance, measured in units of e^2/h , is then given by $g = \text{tr}(\Pi_1 S \Pi_2 S^\dagger)$, where Π_1 is a projection matrix with elements $(\Pi_1)_{j,k} = \delta_{jk}$ for $j \leq n_1$ and zero otherwise and $\Pi_2 = \mathbb{1}_{n_1+n_2} - \Pi_1$. For $\beta = 4$, S matrix has quaternionic entries and Π_1, Π_2 are accordingly modified. The Landauer conductance is equivalently described in terms of the transmission eigenvalues ($0 \leq T_1, \dots, T_n \leq 1$) as [45, 69, 70]

$$g = \sum_{j=1}^n T_j, \quad (15)$$

where $n = \min(n_1, n_2)$. We also define $m = \max(n_1, n_2)$. The joint PDF describing the transmission eigenvalues is given by [45–47, 66, 71]

$$P(T_1, \dots, T_n) \propto \prod_{l=1}^n T_l^a \prod_{1 \leq j < k \leq n} |T_k - T_j|^\beta, \quad (16)$$

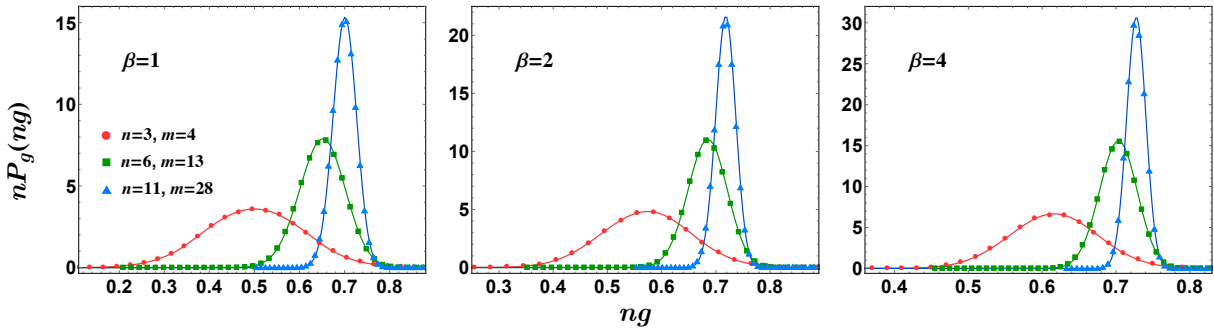


FIG. 3. Distribution of the Landauer conductance for $\beta = 1, 2, 4$ and three combinations of the number of channels n_1, n_2 , as indicated.

where $a = \beta(m-n+1)/2-1$. The above is a special case of the Jacobi ensemble of random matrices [1, 66, 71]. It should be noted that the exponent a is an integer for $\beta = 2, 4$ for any number of channels n_1, n_2 , whereas for $\beta = 1$ we require $|n_1 - n_2|$ to be an odd integer. The distribution of the Landauer conductance follows as

$$P_g(g) = \int_0^1 dT_1 \cdots \int_0^1 dT_n \delta \left(g - \sum_{j=1}^n T_j \right) P(T_1, \dots, T_n). \quad (17)$$

A simple scaling $y_j = T_j/g$ reveals that the above can be written in terms of the CDF of the largest eigenvalue of the fixed trace Wishart-Laguerre ensemble [20],

$$P_g(g) = \frac{1}{\Gamma(\gamma)} K g^{\gamma-1} Q_F(1/g); \quad (18)$$

$$K = \prod_{l=0}^{n-1} \frac{\Gamma\left(a + \frac{\beta(n+l-1)}{2} + 2\right)}{\Gamma\left(\frac{\beta l}{2} + 1\right)}. \quad (19)$$

Plugging in the expression for Q_F from Eq. (9) gives

$$P_g(g) = K \sum_{j=0}^n \Theta(g-j) \times \sum_{k=0}^{ja+j(n-j)\beta} \frac{d_{jk}}{\Gamma(\gamma-k)} \left(\frac{2}{\beta}\right)^k (g-j)^{\gamma-k-1}. \quad (20)$$

This equation provides the sought exact Landauer conductance distribution for general non-negative integer a , β . Corresponding Mathematica code is provided in the Appendix II. In Fig. 3, as examples, we show the distribution of scaled conductance, viz., $nP_g(ng)$ vs. ng for $\beta = 1, 2, 4$ and various n, m combinations. The numerical results obtained using simulation of scattering matrices from circular ensembles are overlaid as symbols on the solid curves based on analytical results. We can see a perfect agreement.

Summary and conclusion. — In this work, we have provided an efficient recursive scheme for the exact com-

putation of the largest eigenvalue distribution of the integer β -Wishart-Laguerre ensemble. Applications to multiple channel communication, bipartite entanglement problems, and an exact solution to the Landauer conductance distribution in a chaotic mesoscopic cavity with ideal leads have been highlighted.

We would like to conclude by emphasizing that the recursive approach proposed in this work for the Wishart-Laguerre largest eigenvalue can be obtained from the more general case of the Jacobi ensemble [42, 43]. The details of this, and its consequences, are planned for a future work.

P.J.F. acknowledges support from the Australian Research Council (ARC) through the ARC Centre of Excellence for Mathematical and Statistical frontiers (ACEMS) and ARC grant DP170102028. S.K. acknowledges the support by the grant EMR/2016/000823 provided by SERB, DST, Government of India. Comments by Mario Kieburg on an earlier draft of the manuscript are appreciated.

* pjforr@unimelb.edu.au

† skumar.physics@gmail.com

- [1] P. J. Forrester, *Log-Gases and Random Matrices* (LMS-34) (Princeton University Press, Princeton, NJ, 2010).
- [2] M. L. Mehta, *Random Matrices* (Academic Press, New York, 2004).
- [3] *Handbook of Random Matrix Theory*, edited by G. Akemann, J. Baik, and P. Di Francesco (Oxford Press, New York, 2011).
- [4] A. G. Constantine, Ann. Math. Statist. **34**, 1270 (1963).
- [5] T. W. Anderson, Ann. Math. Statist. **34**, 122 (1963).
- [6] C. G. Khatri, Ann. Stat. Math. **35**, 1807 (1964).
- [7] R. J. Muirhead, *Aspects of Multivariate Statistical Theory* (Wiley, New York, 1982).
- [8] P. J. Forrester, Nucl. Phys. B **402**, 709 (1993).
- [9] P. J. Forrester, J. Phys. Math. **35**, 2539 (1994).
- [10] P. J. Forrester and T. D. Hughes, J. Phys. Math. **35**, 6739 (1994).
- [11] T. Nagao and P. J. Forrester, Nucl. Phys. B. **509**, 561 (1998).

- [12] K. Johansson, *Commun. Math. Phys.* **209**, 437 (2000).
- [13] I. M. Johnstone, *Ann. Statist.* **29**, 295 (2001).
- [14] P. J. Forrester, *J.Phys. A: Math. Theor.* **40**, 11093 (2007).
- [15] T. Wirtz and T. Guhr, *Phys. Lett. Rev.* **111**, 094101 (2013).
- [16] S. N. Majumdar, O. Bohigas, and A. Lakshminarayan, *J. Stat. Phys.* **131**, 33 (2008).
- [17] G. Akemann and P. Vivo, *J. Stat. Mech.: Theory Exp.* **2011**, P05020 (2011).
- [18] S. N. Majumdar, Extreme Eigenvalues of Wishart Matrices: Application to Entangled Bipartite System, in *The Oxford Handbook of Random Matrix Theory*, edited by G. Akemann, J. Baik, and P. Di Francesco (Oxford University Press, Oxford, 2011).
- [19] S. Kumar, B. Sambasivam, and S. Anand, *J. Phys. A: Math. Theor.* **50**, 345201 (2017).
- [20] P. Vivo, *J. Stat. Mech.: Theory Exp.* **2011**, P01022 (2011).
- [21] M. Kang and M.-S. Alouini, *IEEE J. Sel. Areas Commun.* **21**, 418 (2003).
- [22] P. A. Dighe, R. K. Mallik, and S. S. Jamuar, *IEEE Trans. Commun.* **51**, 694 (2003).
- [23] A. Maaref and S. Aïssa, *IEEE Tran. Commun* **53**, 1092 (2005).
- [24] L. Wei, O. Tirkkonen, P. Dharmawansa and M. McKay, 2012 IEEE International Conference on Communications, 2012.
- [25] C. S. Park and K. B. Lee, *IEEE Tran. Wireless Commun.* **7**, 4432 (2008).
- [26] A. Zanella, M. Chiani, and M. Z. Win, *IEEE Trans. Commun.* **57**, 1050 (2009).
- [27] L. Wei and O. Tirkkonen, *IEEE Int. Conf. Commun. (ICC)*, 2011
- [28] A. Kortun, M. Sellathurai, T. Ratnarajah, and C. Zhong, *IEEE Trans. Signal Process.* **60**, 5527 (2012).
- [29] S. R. Jones, S. D. Howard, I. V. L. Clarkson, K. S. Bialkowski, and D. Cochran, 2017 IEEE International Conference on Acoustics, Speech and Signal Processing (ICASSP)
- [30] C. A. Tracy and H. Widom, *Phys. Lett. B* **305**, 115 (1993).
- [31] C. A. Tracy and H. Widom, *Commun. Phys. Math.* **159**, 151 (1994).
- [32] C. A. Tracy and H. Widom, *Commun. Phys. Math.* **161**, 289 (1994).
- [33] O. N. Feldheim and S. Sodin, *Geom. Funct. Anal.* **20**, 88 (2010).
- [34] P. Vivo, S. N. Majumdar and O. Bohigas, *J. Phys. A: Math. Theor.* **40**, 4317 (2007).
- [35] S. N. Majumdar and M. Vergassola, *Phys. Rev. Lett.* **102**, 060601 (2009).
- [36] E. Katzav and I. P. Castillo, *Phys. Rev. E* **82**(R), 040104 (2010).
- [37] P. J. Forrester, *J. Phys. A: Math. Theor.* **45**, 145201 (2012).
- [38] A. Edelman, *Eigenvalues and condition numbers of random matrices*, Ph.D. thesis MIT 1989.
- [39] A. Edelman, *Lin. Alg. Appl.* **159**, 55 (1991).
- [40] P. J. Forrester, *J. Stat. Phys.* **72**, 39 (1993).
- [41] P. J. Forrester and M. Ito, *J. Phys. A: Math. Theor.* **43**, 175202 (2010).
- [42] P. J. Forrester and E. M. Rains, *Commun. Math. Phys.* **309**, 771 (2012).
- [43] P. J. Forrester and A. K. Trinh, *Nucl. Phys. B*, **938**, 621 (2019).
- [44] S. Kumar, *J. Stat. Phys.* **175**, 126 (2019).
- [45] C. W. J. Beenakker, *Rev. Mod. Phys.* **69**, 731 (1997).
- [46] H. U. Baranger and P. A. Mello, *Phys. Rev. Lett.* **73**, 142 (1994).
- [47] R. A. Jalabert, J.-L. Pichard, and C. W. J. Beenakker, *Europhys. Lett.* **27**, 255 (1994).
- [48] P. A. Mello and N. Kumar, *Quantum Transport in Mesoscopic Systems* (Oxford University Press, 2004).
- [49] H.-J. Sommers, W. Wieczorek, and D.V. Savin, *Acta Phys. Pol. A* **112**, 691 (2007).
- [50] B. A. Khoruzhenko, D. V. Savin, and H.-J. Sommers, *Phys. Rev. B* **80**, 125301 (2009).
- [51] S. Kumar and A. Pandey, *J. Phys. A: Math. Theor.* **43**, 285101 (2010).
- [52] D. E. Johnson and F. A. Graybill, *J. Amer. Stat. Assoc.*, **67**, 862 (1972).
- [53] A. W. Davis, *J. Mult. Anal.* **2**, 440 (1972).
- [54] F. J. Schurmann, P. R. Krishnaiah and A. K. Chattopadhyay, *J. Mult. Anal.* **3**, 445 (1973).
- [55] P. R. Krishnaiah and F. J. Schurmann, *J. Multi. Anal.* **4**, 265 (1974).
- [56] O. Besson and L.L. Scharf, *IEEE Trans. Signal Process.* **54**, 2840 (2006).
- [57] P. Bianchi, M. Debbah, M. Maida and J. Najim, *IEEE Trans. Inf. Th.* **57**, 2400 (2011).
- [58] B. Nadler, *J. Multivariate Analysis.* **102**, 363 (2011).
- [59] K. Życzkowski and H.-J. Sommers, *J. Math. Phys.: Math. Gen* **34**, 7111 (2001).
- [60] A. T. James, *Special functions of matrix and single argument in statistics*, in *Theory and Applications of Special Functions* (R. A. Askey, Ed.), Academic, New York, 1975, pp. 497-520
- [61] Wolfram Research Inc. *Mathematica* Version 11.0 (2016).
- [62] Y. Imry, *Europhys. Lett.* **1**, 249 (1986).
- [63] B. L. Altshuler and B. I. Shklovskii, *Zh. Eksp. Teor. Fiz.* **91**, 220 (1986); *Sov. Phys. JETP* **64**, 127 (1986).
- [64] A. D. Stone, P. A. Mello, K. A. Muttalib, and J.-L. Pichard, in *Mesoscopic Phenomena in Solids*, edited by B. L. Altshuler, P. A. Lee, and R. A. Webb (North-Holland, Amsterdam, 1991): p. 369.
- [65] C. W. J. Beenakker, *Rev. Mod. Phys.* **87**, 1037 (2015).
- [66] P. J. Forrester, *J. Phys. A: Math. Gen.* **39**, 6861 (2006).
- [67] P. W. Brouwer, *Phys. Rev. B* **51**, 16878 (1995).
- [68] P. Vidal and E. Kanzieper, *Phys. Rev. Lett.* **108**, 206806 (2012).
- [69] R. Landauer, *IBM J. Res. Dev.* **1**, 223 (1957).
- [70] D. S. Fisher and P. A. Lee, *Phys. Rev. B* **23**, 6851 (1981).
- [71] S. Kumar and A. Pandey, *J. Phys. A: Math. Theor.* **43**, 085001 (2010).

APPENDICES

APPENDIX I. REFINEMENT OF UPPER LIMIT OF INNER SUMMATION IN EQ. (6)

We discuss here the refinement of the upper limit of inner summation in Eq. (6). For this we consider the j -point correlation function,

$$\rho_{(j)}(x_1, \dots, x_j) = \frac{n!}{(n-j)!} \times \int_0^\infty dx_{j+1} \cdots \int_0^\infty dx_n \mathcal{P}(x_1, \dots, x_n), \quad (\text{A1})$$

and the following expansion of $Q(x)$ in terms of $\rho_{(j)}$:

$$Q(x) = 1 + \sum_{j=1}^n \frac{(-1)^j}{j!} \int_x^\infty dx_1 \cdots \int_x^\infty dx_j \rho_{(j)}(x_1, \dots, x_j). \quad (\text{A2})$$

We then use the fact that for large x_1, \dots, x_j , $\rho_{(j)}(x_1, \dots, x_j)$ is proportional to

$$\prod_{l=1}^j x_l^{a+\beta(n-j)} e^{-\beta x_l/2} \prod_{1 \leq p < q \leq j} |x_p - x_q|^\beta. \quad (\text{A3})$$

and perform integration by parts multiple times to effectively eliminate the product of differences. The latter procedure reveals, for each j , the exponent κ in the leading large x form $x^\kappa e^{-\beta j x/2}$ and thus the upper limit in the summation over k in Eq. (6). The value $\kappa = ja + j(n-j)\beta$ is obtained, as appears in Eq. (6).

APPENDIX II. DESCRIPTION OF THE MATHEMATICA CODE

We implement the proposed recursion scheme in a Mathematica code which is provided below.

From the discussion of the recursion scheme, it follows that we need a three level nested loop to obtain the expressions for the PDF $P(x)$ and CDF $Q(x)$. Since the overall expression for a given dimension n builds upon

the lower values of dimension, the outermost loop runs over $\nu = 1, 2, \dots, n-1$. At a given ν value, the innermost loop involves recursion over p as in Eq. (14) from $p = 0$ to $\nu-1$, so as to increase the exponent α by 1. The α , overall, needs to be iterated from 0 to $\beta-1$ so as to obtain the result for a given β . This is achieved in the middle loop. Once these three loops are completed, the expression for $P(x)$ is obtained. A final integration is then performed (corresponding to $\nu = n$) to yield the corresponding $Q(x)$.

The algorithm involves performing integral over expressions containing linear combination of terms like $x^r e^{-sx}$ (Laguerre weight) several times. We found that the direct use of the inbuilt function ‘Integrate’ in Mathematica is extremely inefficient at performing this task if there are many terms in the expression. Therefore, we use the ‘Map’ ($/@$) function and apply the result in Eq. (12) to individual terms in the expression and thereby obtain the overall integrated result in view of the linearity.

The coefficients c_{jk} and d_{jk} are extracted readily from the obtained $P(x)$ and $Q(x)$ expressions with the aid of the ‘CoefficientList’ function in Mathematica. These are then used to yield explicit expressions for the PDF $P_F(y)$ and CDF $Q_F(y)$ for the fixed trace ensemble and also the Landauer conductance density function $P_g(g)$. It should be noted that in Mathematica list indices start from 1 and not from 0, therefore the indices in the Eqs. (5), (6), (8), (9) and (20) are accordingly shifted when implemented in the code.

From Eqs. (5) and (6) it is clear that there are $(n/6)[(n^2-1)\beta + 3(n-1)a + 6]$ and $(1/6)(n+1)[n^2\beta + n(3a - \beta) + 6]$ terms in the expanded expressions of $P(x)$ and $Q(x)$, respectively. As a consequence, the symbolic expressions become very lengthy even for moderate values of n and a . For example, if we consider $\beta = 2, n = 5, a = 5$, the number of terms in the expanded expressions comes out to 95 and 121, respectively. For numerical evaluation of such lengthy expressions we must work with a very high precision so as to prevent under- or over-flow.

The above described three level nested loop algorithm may be contrasted with that for the smallest eigenvalue [44], which involves a two level nested loop only due to a less involved mathematical structure there.

Mathematica code for computation of β - Wishart Laguerre largest eigenvalue distribution and Landauer conductance distribution

Parameters:

Enter the parameters here for β - Wishart Laguerre largest eigenvalue distribution.
 n should be greater than 1.

```
In[1]:= β = 2; n = 3; a = 5;
```

Enter the parameters below instead for Landauer conductance distribution.
 $|n1-n2|$ should be an odd integer if β is odd, and $\min(n1,n2)$ should be greater than 1.

```
In[2]:= β = 2; n1 = 3; n2 = 8;
```

```
n = Min[n1, n2]; m = Max[n1, n2];
a = β (m - n + 1) / 2 - 1;
```

Recursion scheme:

```
γ = n (a + β (n - 1) / 2 + 1);
int[c_, a_, b_] := c a! / b^(a+1) (1 - E^-b Sum[(b x)^k / k!, {k, 0, a}]);
winv[n_, β_, a_] :=
  Binomial[β^n (β (n-1)/2+a+1), Gamma[β/2+1]] / (Gamma[β (j+1)/2+1] Gamma[β j/2+a+1]);
L[-1] = 0; L[0] = int[1, a, β/2];

Monitor[For[v = 1, v ≤ n - 1, v++, {
  For[α = 0, α ≤ β - 1, α++, {
    For[p = 0, p ≤ v - 1, p++, {
      L[p + 1] = 2 / β (v - p) ((β/2 (v - p) x + (p - v) (a + α + 1 + β/2 (v - p - 1))) L[p] +
        x D[L[p], x] - p (β/2 (v - p) + α + 1) x L[p - 1]) // Expand;
    }];
    L[0] = L[v];
    L[-1] = 0;
  }];
  L[0] =
    Expand[(v + 1) int[FactorTermsList[#, x][[1]], Exponent[#, x] + a, Exponent[#, E^-x] + β/2] & /@
      Expand[L[v]]];
}, {v, α, p}];
```

Expressions for the PDF and CDF of the largest eigenvalue of the unrestricted trace ensemble:

These are the expressions of $P(x)$ and $Q(x)$ in fully expanded form, as obtained directly from the recursion.

```
In[5]:= Px[x_] = Expand[n winv[n, β, a] x^a e^{-β x/2} L[n - 1]];
Qx[x_] = Expand[int[FactorTermsList[#, x][[1]], Exponent[#, x], Exponent[#, e^{-x}]] & /@ Px[x]];
```

Extraction of the coefficients c_{jk} and d_{jk} :

```
In[6]:= c = Take[CoefficientList[CoefficientList[Px[x], e^{-β x/2}], x], {2, n + 1}];
d = Take[CoefficientList[CoefficientList[Qx[x], e^{-β x/2}], x], {1, n + 1}];
```

Expressions for the PDF and CDF of the largest eigenvalue of the unrestricted trace ensemble expanded as in Eqs. (5) and (6):

These are based on rewriting the expressions for $P(x)$ and $Q(x)$ using the extracted coefficients.

```
In[7]:= P[x_] = Sum[e^{-j β x/2} (Sum[c[[j, k]] x^{k-1}, {k, a+1, j (β (n-j) + a) + 1}], {j, 1, n}];
Q[x_] = Sum[e^{-(j-1) β x/2} (Sum[d[[j, k]] x^{k-1}, {k, 1, (j-1) (β (n-j+1) + a) + 1}], {j, 1, n+1});
```

Expressions for the PDF and CDF of the largest eigenvalue of the fixed trace ensemble:

```
In[8]:= PF[y_] = Sum[HeavisideTheta[1 - j y]
  (Sum[2/β Gamma[γ] c[[j, k]] (2 y/β)^{k-1} (1 - j y)^{γ-k-1}, {k, a+1, j (β (n-j) + a) + 1}], {j, 1, n}];
QF[y_] = Sum[HeavisideTheta[1 - (j-1) y] (Sum[Γ d[[j, k]] (2 y/β)^{k-1} (1 - (j-1) y)^{γ-k},
  {k, 1, (j-1) (β (n-j+1) + a) + 1}], {j, 1, n+1});
```

Expression for the Landauer conductance distribution:

```
In[9]:= Pg[g_] = Product[Γ[a + β/2 (n + l - 1) + 2]/Γ[β/2 l + 1], {l, 0, n - 1}]
  Sum[HeavisideTheta[g - (j - 1)] (Sum[d[[j, k]] (2/β)^{k-1} (g - (j - 1))^γ-k,
  {k, 1, (j - 1) (a + β (n - j + 1)) + 1}], {j, 1, n + 1});
```

Example computations:

The following print the quantities computed above.

In[6]:= P[x]

$$\begin{aligned} \text{Out[6]:= } & e^{-x} \left(\frac{7x^5}{30} - \frac{2x^6}{15} + \frac{7x^7}{240} - \frac{x^8}{360} + \frac{x^9}{10080} \right) + \\ & e^{-2x} \left(-\frac{7x^5}{15} - \frac{x^6}{5} - \frac{x^7}{40} + \frac{x^8}{360} + \frac{x^9}{840} + \frac{x^{10}}{12600} - \frac{x^{11}}{33600} - \frac{x^{12}}{100800} + \frac{x^{13}}{1209600} - \frac{x^{14}}{3628800} \right) + e^{-3x} \\ & \left(\frac{7x^5}{30} + \frac{x^6}{3} + \frac{11x^7}{48} + \frac{x^8}{10} + \frac{103x^9}{3360} + \frac{173x^{10}}{25200} + \frac{17x^{11}}{15120} + \frac{x^{12}}{7560} + \frac{13x^{13}}{1209600} + \frac{x^{14}}{1814400} + \frac{x^{15}}{72576000} \right) \end{aligned}$$

In[6]:= Q[x]

$$\begin{aligned} \text{Out[6]:= } & 1 + e^{-x} \left(-3 - 3x - \frac{3x^2}{2} - \frac{x^3}{2} - \frac{x^4}{8} - \frac{x^5}{40} + \frac{5x^6}{144} - \frac{71x^7}{5040} + \frac{19x^8}{10080} - \frac{x^9}{10080} \right) + \\ & e^{-2x} \left(3 + 6x + 6x^2 + 4x^3 + 2x^4 + \frac{4x^5}{5} + \frac{17x^6}{90} + \frac{8x^7}{315} + \frac{13x^8}{4032} + \right. \\ & \left. \frac{31x^9}{30240} + \frac{7x^{10}}{21600} + \frac{x^{11}}{15120} + \frac{31x^{12}}{3628800} + \frac{x^{13}}{1814400} + \frac{x^{14}}{7257600} \right) + \\ & e^{-3x} \left(-1 - 3x - \frac{9x^2}{2} - \frac{9x^3}{2} - \frac{27x^4}{8} - \frac{81x^5}{40} - \frac{701x^6}{720} - \frac{207x^7}{560} - \frac{739x^8}{6720} - \frac{103x^9}{4032} - \right. \\ & \left. \frac{103x^{10}}{22400} - \frac{127x^{11}}{201600} - \frac{463x^{12}}{7257600} - \frac{11x^{13}}{2419200} - \frac{x^{14}}{4838400} - \frac{x^{15}}{217728000} \right) \end{aligned}$$

In[6]:= PF[y]

$$\begin{aligned} \text{Out[6]:= } & (16959096 (1 - 3y)^{17} y^5 + 411863760 (1 - 3y)^{16} y^6 + 4530501360 (1 - 3y)^{15} y^7 + \\ & 29654190720 (1 - 3y)^{14} y^8 + 127265901840 (1 - 3y)^{13} y^9 + 370512638496 (1 - 3y)^{12} y^{10} + \\ & 728175127680 (1 - 3y)^{11} y^{11} + 942344282880 (1 - 3y)^{10} y^{12} + 765654729840 (1 - 3y)^9 y^{13} + \\ & 353379106080 (1 - 3y)^8 y^{14} + 70675821216 (1 - 3y)^7 y^{15}) \text{HeavisideTheta}[1 - 3y] + \\ & (-33918192 (1 - 2y)^{17} y^5 - 247118256 (1 - 2y)^{16} y^6 - 494236512 (1 - 2y)^{15} y^7 + \\ & 823727520 (1 - 2y)^{14} y^8 + 4942365120 (1 - 2y)^{13} y^9 + 4283383104 (1 - 2y)^{12} y^{10} - \\ & 19275223968 (1 - 2y)^{11} y^{11} - 70675821216 (1 - 2y)^{10} y^{12} + \\ & 58896517680 (1 - 2y)^9 y^{13} - 176689553040 (1 - 2y)^8 y^{14}) \text{HeavisideTheta}[1 - 2y] + \\ & (16959096 (1 - y)^{17} y^5 - 164745504 (1 - y)^{16} y^6 + 576609264 (1 - y)^{15} y^7 - \\ & 823727520 (1 - y)^{14} y^8 + 411863760 (1 - y)^{13} y^9) \text{HeavisideTheta}[1 - y] \end{aligned}$$

In[5]:= QF[y]

$$\begin{aligned}
Out[5]= & 1 + \left(- (1 - 3 y)^{23} - 69 (1 - 3 y)^{22} y - 2277 (1 - 3 y)^{21} y^2 - 47817 (1 - 3 y)^{20} y^3 - 717255 (1 - 3 y)^{19} y^4 - \right. \\
& 8176707 (1 - 3 y)^{18} y^5 - 70763847 (1 - 3 y)^{17} y^6 - 456727491 (1 - 3 y)^{16} y^7 - \\
& 2174052276 (1 - 3 y)^{15} y^8 - 7575351300 (1 - 3 y)^{14} y^9 - 19089885276 (1 - 3 y)^{13} y^{10} - \\
& 33999353388 (1 - 3 y)^{12} y^{11} - 41316799524 (1 - 3 y)^{11} y^{12} - 32393084724 (1 - 3 y)^{10} y^{13} - \\
& 14724129420 (1 - 3 y)^9 y^{14} - 2944825884 (1 - 3 y)^8 y^{15} \Big) \text{HeavisideTheta}[1 - 3 y] + \\
& \left(3 (1 - 2 y)^{23} + 138 (1 - 2 y)^{22} y + 3036 (1 - 2 y)^{21} y^2 + 42504 (1 - 2 y)^{20} y^3 + \right. \\
& 425040 (1 - 2 y)^{19} y^4 + 3230304 (1 - 2 y)^{18} y^5 + 13728792 (1 - 2 y)^{17} y^6 + \\
& 31380096 (1 - 2 y)^{16} y^7 + 63740820 (1 - 2 y)^{15} y^8 + 303994680 (1 - 2 y)^{14} y^9 + \\
& 1345421616 (1 - 2 y)^{13} y^{10} + 3569485920 (1 - 2 y)^{12} y^{11} + 5532703176 (1 - 2 y)^{11} y^{12} + \\
& 3926434512 (1 - 2 y)^{10} y^{13} + 9816086280 (1 - 2 y)^9 y^{14} \Big) \text{HeavisideTheta}[1 - 2 y] + \\
& \left(-3 (1 - y)^{23} - 69 (1 - y)^{22} y - 759 (1 - y)^{21} y^2 - 5313 (1 - y)^{20} y^3 - 26565 (1 - y)^{19} y^4 - \right. \\
& 100947 (1 - y)^{18} y^5 + 2523675 (1 - y)^{17} y^6 - 17406147 (1 - y)^{16} y^7 + \\
& 37263864 (1 - y)^{15} y^8 - 29418840 (1 - y)^{14} y^9 \Big) \text{HeavisideTheta}[1 - y]
\end{aligned}$$

In[6]:= Pg[g]

$$\begin{aligned}
Out[6]= & 26547069911040000 \\
& \left(\left(- \frac{(-3 + g)^8}{8778792960000} - \frac{(-3 + g)^9}{1755758592000} - \frac{11 (-3 + g)^{10}}{8778792960000} - \frac{463 (-3 + g)^{11}}{289700167680000} - \right. \right. \\
& \frac{127 (-3 + g)^{12}}{96566722560000} - \frac{103 (-3 + g)^{13}}{139485265920000} - \frac{103 (-3 + g)^{14}}{351502870118400} - \frac{739 (-3 + g)^{15}}{8787571752960000} - \\
& \frac{23 (-3 + g)^{16}}{1301862481920000} - \frac{701 (-3 + g)^{17}}{256094948229120000} - \frac{(-3 + g)^{18}}{3161666027520000} - \\
& \frac{(-3 + g)^{19}}{36042992713728000} - \frac{(-3 + g)^{20}}{540644890705920000} - \frac{(-3 + g)^{21}}{11353542704824320000} - \\
& \left. \left. \frac{(-3 + g)^{22}}{374666909259202560000} - \frac{(-3 + g)^{23}}{25852016738884976640000} \right) \text{HeavisideTheta}[-3 + g] + \right. \\
& \left(\frac{(-2 + g)^9}{2633637888000} + \frac{(-2 + g)^{10}}{6584094720000} + \frac{31 (-2 + g)^{11}}{144850083840000} + \frac{(-2 + g)^{12}}{7242504192000} + \right. \\
& \frac{(-2 + g)^{13}}{19214807040000} + \frac{31 (-2 + g)^{14}}{2636271525888000} + \frac{(-2 + g)^{15}}{405580234752000} + \\
& \frac{(-2 + g)^{16}}{823834851840000} + \frac{(-2 + g)^{17}}{1883051089920000} + \frac{(-2 + g)^{18}}{8002967132160000} + \\
& \frac{(-2 + g)^{19}}{60822550204416000} + \frac{(-2 + g)^{20}}{608225502044160000} + \frac{(-2 + g)^{21}}{8515157028618240000} + \\
& \left. \left. \frac{(-2 + g)^{22}}{187333454629601280000} + \frac{(-2 + g)^{23}}{8617338912961658880000} \right) \text{HeavisideTheta}[-2 + g] + \right. \\
& \left(- \frac{(-1 + g)^{14}}{878757175296000} + \frac{19 (-1 + g)^{15}}{13181357629440000} - \frac{71 (-1 + g)^{16}}{105450861035520000} + \right. \\
& \frac{(-1 + g)^{17}}{10243797929164800} - \frac{(-1 + g)^{18}}{256094948229120000} - \frac{(-1 + g)^{19}}{973160803270656000} - \\
& \frac{(-1 + g)^{20}}{4865804016353280000} - \frac{(-1 + g)^{21}}{34060628114472960000} - \frac{(-1 + g)^{22}}{374666909259202560000} - \\
& \left. \left. \frac{(-1 + g)^{23}}{8617338912961658880000} \right) \text{HeavisideTheta}[-1 + g] + \frac{g^{23} \text{HeavisideTheta}[g]}{25852016738884976640000} \right)
\end{aligned}$$

High precision numerical evaluation of P(x) and Q(x) and their plots:

P(x) and Q(x) are numerically evaluated below with 6-digit precision in the interval [2, 28] with a step size 1/4. Other expressions obtained above can be similarly evaluated. Please use integers or fractions for entering the interval and step size in order to maintain precision. 'MaxExtraPrecision' option used below may be increased to a higher value in case of a precision loss.

Exact symbolic results may also be obtained by removing the numerical value (N) option and directly printing {x,P[x]} if exact x is supplied.

```
In[=]:= PxN =
Monitor[Table[{N[x], Block[{$MaxExtraPrecision = 10000}, N[Px[x], 6]]}, {x, 2, 28, 1/4}], x]

Out[=]= {{2., 8.64138*10^-11}, {2.25, 7.49194*10^-10}, {2.5, 4.89239*10^-9}, {2.75, 2.54134*10^-8}, {3., 1.09326*10^-7}, {3.25, 4.01595*10^-7}, {3.5, 1.29001*10^-6}, {3.75, 3.69259*10^-6}, {4., 9.56315*10^-6}, {4.25, 0.0000226886}, {4.5, 0.0000498224}, {4.75, 0.000102141}, {5., 0.000196929}, {5.25, 0.000359298}, {5.5, 0.000623686}, {5.75, 0.00103481}, {6., 0.00164779}, {6.25, 0.00252715}, {6.5, 0.00374463}, {6.75, 0.00537581}, {7., 0.00749570}, {7.25, 0.0101736}, {7.5, 0.0134677}, {7.75, 0.0174199}, {8., 0.0220514}, {8.25, 0.0273591}, {8.5, 0.0333137}, {8.75, 0.0398589}, {9., 0.0469132}, {9.25, 0.0543717}, {9.5, 0.0621107}, {9.75, 0.0699923}, {10., 0.0778697}, {10.25, 0.0855933}, {10.5, 0.0930163}, {10.75, 0.100000}, {11., 0.106418}, {11.25, 0.112161}, {11.5, 0.117138}, {11.75, 0.121279}, {12., 0.124538}, {12.25, 0.126888}, {12.5, 0.128324}, {12.75, 0.128861}, {13., 0.128530}, {13.25, 0.127379}, {13.5, 0.125466}, {13.75, 0.122861}, {14., 0.119639}, {14.25, 0.115880}, {14.5, 0.111667}, {14.75, 0.107082}, {15., 0.102204}, {15.25, 0.0971113}, {15.5, 0.0918751}, {15.75, 0.0865623}, {16., 0.0812332}, {16.25, 0.0759416}, {16.5, 0.0707345}, {16.75, 0.0656522}, {17., 0.0607281}, {17.25, 0.0559897}, {17.5, 0.0514583}, {17.75, 0.0471499}, {18., 0.0430757}, {18.25, 0.0392421}, {18.5, 0.0356520}, {18.75, 0.0323047}, {19., 0.0291971}, {19.25, 0.0263232}, {19.5, 0.0236755}, {19.75, 0.0212448}, {20., 0.0190210}, {20.25, 0.0169930}, {20.5, 0.0151492}, {20.75, 0.0134780}, {21., 0.0119673}, {21.25, 0.0106056}, {21.5, 0.00938124}, {21.75, 0.00828319}, {22., 0.00730077}, {22.25, 0.00642385}, {22.5, 0.00564284}, {22.75, 0.00494875}, {23., 0.00433319}, {23.25, 0.00378836}, {23.5, 0.00330709}, {23.75, 0.00288275}, {24., 0.00250928}, {24.25, 0.00218118}, {24.5, 0.00189342}, {24.75, 0.00164145}, {25., 0.00142119}, {25.25, 0.00122894}, {25.5, 0.00106139}, {25.75, 0.000915593}, {26., 0.000788898}, {26.25, 0.000678958}, {26.5, 0.000583687}, {26.75, 0.000501237}, {27., 0.000429974}, {27.25, 0.000368458}, {27.5, 0.000315420}, {27.75, 0.000269747}, {28., 0.000230462}}
```

```
In[1]:= ListLinePlot[PxN, AxesLabel -> {"x", "P(x)"}, PlotStyle -> Red,
LabelStyle -> {15, Black}, Background -> RGBColor[1, 0.95, 0.95]]
```

```
Out[1]=
```

```
In[2]:= QxN =
Monitor[Table[{N[x], Block[{$MaxExtraPrecision = 10000}, N[Q[x], 6]]}, {x, 2, 28, 1/4}], x]
```

```
Out[2]= {{2., 8.72823 \times 10^{-12}}, {2.25, 8.73405 \times 10^{-11}}, {2.5, 6.50414 \times 10^{-10}}, {2.75, 3.81578 \times 10^{-9}}, {3., 1.83933 \times 10^{-8}}, {3.25, 7.52135 \times 10^{-8}}, {3.5, 2.67469 \times 10^{-7}}, {3.75, 8.43620 \times 10^{-7}}, {4., 2.39778 \times 10^{-6}}, {4.25, 6.22164 \times 10^{-6}}, {4.5, 0.0000148972}, {4.75, 0.0000332147}, {5., 0.0000694851}, {5.25, 0.000137285}, {5.5, 0.000257607}, {5.75, 0.000461327}, {6., 0.000791808}, {6.25, 0.00130740}, {6.5, 0.00208355}, {6.75, 0.00321419}, {7., 0.00481219}, {7.25, 0.00700857}, {7.5, 0.00995039}, {7.75, 0.0137973}, {8., 0.0187170}, {8.25, 0.0248795}, {8.5, 0.0324506}, {8.75, 0.0415856}, {9., 0.0524225}, {9.25, 0.0650759}, {9.5, 0.0796318}, {9.75, 0.0961432}, {10., 0.114628}, {10.25, 0.135065}, {10.5, 0.157399}, {10.75, 0.181537}, {11., 0.207352}, {11.25, 0.234689}, {11.5, 0.263368}, {11.75, 0.293189}, {12., 0.323935}, {12.25, 0.355382}, {12.5, 0.387302}, {12.75, 0.419469}, {13., 0.451660}, {13.25, 0.483665}, {13.5, 0.515286}, {13.75, 0.546341}, {14., 0.576665}, {14.25, 0.606115}, {14.5, 0.634567}, {14.75, 0.661918}, {15., 0.688084}, {15.25, 0.713002}, {15.5, 0.736628}, {15.75, 0.758933}, {16., 0.779908}, {16.25, 0.799553}, {16.5, 0.817885}, {16.75, 0.834931}, {17., 0.850725}, {17.25, 0.865310}, {17.5, 0.878737}, {17.75, 0.891058}, {18., 0.902331}, {18.25, 0.912616}, {18.5, 0.921973}, {18.75, 0.930462}, {19., 0.938145}, {19.25, 0.945080}, {19.5, 0.951325}, {19.75, 0.956936}, {20., 0.961965}, {20.25, 0.966463}, {20.5, 0.970477}, {20.75, 0.974052}, {21., 0.977229}, {21.25, 0.980048}, {21.5, 0.982544}, {21.75, 0.984749}, {22., 0.986695}, {22.25, 0.988408}, {22.5, 0.989915}, {22.75, 0.991237}, {23., 0.992396}, {23.25, 0.993409}, {23.5, 0.994295}, {23.75, 0.995068}, {24., 0.995741}, {24.25, 0.996326}, {24.5, 0.996835}, {24.75, 0.997276}, {25., 0.997658}, {25.25, 0.997989}, {25.5, 0.998275}, {25.75, 0.998521}, {26., 0.998734}, {26.25, 0.998917}, {26.5, 0.999075}, {26.75, 0.999210}, {27., 0.999326}, {27.25, 0.999426}, {27.5, 0.999511}, {27.75, 0.999584}, {28., 0.999647}}
```

```
In[6]:= ListLinePlot[QxN, AxesLabel -> {"x", "Q(x)"}, PlotStyle -> Blue,
LabelStyle -> {15, Black}, Background -> RGBColor[0.9, 0.98, 1]]
```

